



1 Extending flood forecasting lead time in large watershed by coupling WRF QPF with
2 distributed hydrological model

3 Ji Li¹, Yangbo Chen¹, Huanyu Wang¹, Jianming Qin¹, Jie Li²

4 ¹Department of Water Resources and Environment, Sun Yat-sen University,
5 Guangzhou 510275, China

6 ²Hydrology Bureau, Pearl River Water Resources Commission, Guangzhou 510370,
7 China

8

9 *Correspondence to:* Yangbo Chen (eescyb@mail.sysu.edu.cn)

10

11 **Abstract.** Long lead time flood forecasting is very important for large watershed
12 flood mitigation as it provides more time for flood warning and emergency responses.
13 Latest numerical weather forecast model could provide 1-15 days quantitative
14 precipitation forecasting products at grid format, by coupling this product with
15 distributed hydrological model could produce long lead time watershed flood
16 forecasting products. This paper studied the feasibility of coupling the Liuxihe Model
17 with the WRF QPF for a large watershed flood forecasting in southern China. The
18 QPF of WRF products has three lead time, including 24 hour, 48 hour and 72 hour,
19 the grid resolution is 20kmx20km. The Liuxihe Model is set up with freely
20 downloaded terrain property, the model parameters were previously optimized with
21 rain gauge observed precipitation, and re-optimized with WRF QPF. Results show
22 that the WRF QPF has bias with the rain gauge precipitation, and a post-processing
23 method is proposed to post process the WRF QPF products, which improves the flood
24 forecasting capability. With model parameter re-optimization, the model's
25 performance improves also, it suggests that the model parameters be optimized with
26 QPF, not the rain gauge precipitation. With the increasing of lead time, the accuracy
27 of WRF QPF decreases, so does the flood forecasting capability. Flood forecasting
28 products produced by coupling Liuxihe Model with WRF QPF provides good



29 reference for large watershed flood warning due to its long lead time and rational
30 results.

31

32 **Key words :** WRF, Liuxihe Model, Flood forecasting, lead time, parameter
33 optimization

34

35 **1 Introduction**

36 Watershed flood forecasting is one of the most important non-engineering measures
37 for flood mitigation(Tingsanchali, 2012, Li et al., 2002), significant progresses in
38 watershed flood forecasting has been made in the past decades(Borga et al., 2011,
39 Moreno et al., 2013). Lead time is a key index for watershed flood forecasting,
40 especially for large watershed (Toth et al., 2000, Han et al., 2007). Only flood
41 forecasting products with long lead time is useful as it could provide enough time for
42 flood warning and flood emergency responses. In the long practice of flood
43 forecasting, ground based rain gauge measured precipitation is the main input for
44 flood forecasting model, but as this kind of precipitation is the rainfall falling to the
45 ground already, so it has no lead time. This makes the watershed flood forecasting
46 with very short lead time (Jasper et al., 2002), and could not satisfy the requirement of
47 flood warning (Shim et al., 2002) in lead time, particularly in large watershed, thus
48 reducing the value of the flood forecasting products in watershed flood mitigation.

49

50 The developed numerical weather prediction model in the past decades could provide
51 longer lead time quantitative precipitation forecast(QPF) product at grid format, the
52 lead time for the latest weather prediction model could be as long as to 1~15 days



53 (Buizza,1999, Ahlgrimm et al., 2016). By coupling the weather prediction model QPF
54 with flood forecasting model, the flood forecasting lead time thus could be extended,
55 this provides new way for large watershed flood forecasting (Jasper et al., 2002,
56 Zappa et al., 2010, Giard and Bazile, 2000). Many numerical weather prediction
57 models have been proposed and put into operational use, such as the European Centre
58 Medium-Range Weather Forecasts (ECMWF) Ensemble Prediction System (EPS)
59 (Molteni et. al., 1996, Barnier et. al.,1995), the weather research and forecasting
60 (WRF) model (Skamarock, 2005, 2008, Maussion, 2011), the numerical weather
61 forecast model of Japan Meteorological Agency (Takenaka et al., 2011, Gao and Lian,
62 2006), the numerical forecast model of China Meteorological Agency (Li and Chen,
63 2002), and others.

64

65 Watershed flood forecasting relies on hydrological model for computation tool, while
66 the precipitation is the model's driving force. The earliest hydrological model is
67 regarded as the Sherman unit-graph (Sherman, 1932), which belongs to the category
68 of lumped hydrological model. Many lumped hydrological models have been
69 proposed, such as the Sacramento model (Burnash, 1995), the NAM model (DHI,
70 2004), the Xinanjiang model (Zhao, 1977), among others. The lumped hydrological
71 model regards the watershed as a whole hydrological unit, thus the model parameter is
72 the same over the watershed, but this is not true, particularly for a large watershed.
73 The precipitation the lumped hydrological model used is averaged over the watershed
74 also, this further increases the model's uncertainty in large watershed flood
75 forecasting as it is well known that the precipitation distribution over the watershed is
76 highly uneven. The QPF produced by numerical weather prediction model forecasts
77 precipitation at grid format, which provides detailed precipitation distribution



78 information over watershed, it is another advantage of QPF. The lumped hydrological
79 model could not take the advantage of gridded WPF products.

80

81 The latest development of watershed hydrological model is the distributed
82 hydrological model (Refsgaard et. al., 1996), which divides the watershed into grids,
83 and different grids could have their own precipitation, terrain property and model
84 parameter, so distributed hydrological model is the ideal model for coupling WRF
85 QPF for watershed flood forecasting. The first proposed distributed hydrological
86 model is SHE model (Abbott et. al.1986a, 1986b), and now many distributed
87 hydrological models have been proposed, and a few have been used for watershed
88 flood forecasting, such as the SHE model (Abbott et. al.1986a, 1986b), the
89 WATERFLOOD model (Kouwen, 1988), the VIC model (Liang et. al., 1994), the
90 WetSpa model (Wang et. al., 1997), the Vflo model (Vieux et. al., 2002), the WEHY
91 model(Kavvas et al., 2004), the Liuxihe model (Chen et. al., 2009, 2011), among
92 others.

93

94 As distributed hydrological model calculates the hydrological process at grid scale, so
95 the computation time needed for running the distributed hydrological model is huge
96 even for a small watershed, which limits the model's application in watershed flood
97 forecasting, particularly in large watershed. Model parameter uncertainty related to
98 distributed hydrological model also impacted its application. But with the
99 development of parallel computation algorithm for distributed hydrological model
100 and its deployment on supercomputer (Chen et. al., 2013), the computation burden is
101 not a challenge of distributed hydrological modeling anymore. Also with the



102 development of automatical parameter optimization of distributed hydrological model
103 in flood forecasting (Madsen et. al., 2003, Shafii et. al., 2009, Xu et. al., 2012, Chen et.
104 al., 2016), the model parameters could be optimized, and the model's performance
105 could be improved largely. With these advances, now distributed hydrological model
106 could be used for large watershed flood forecasting.

107

108 In this paper, the WRF QPF is coupled with the distributed hydrological model-the
109 Liuxihe model for a large watershed flood forecasting in southern China. The spatial
110 and temporal resolution of WRF QPF is at 20km*20km and 1 hour respectively with
111 three lead time, including 24 hour, 48 hour and 72 hour. The WRF QPF has a similar
112 pattern with that estimated by rain gauges, but overestimates the averaged watershed
113 precipitation, and the longer the WRF QPF lead time, the higher the precipitation
114 overestimation. WRF QPF has systematic bias compared with rain gauge precipitation,
115 a post-processing method is proposed to post process the WRF QPF products, which
116 improves the flood forecasting capability. The Liuxihe Model is set up with freely
117 downloaded terrain property, the model parameters were previously optimized with
118 rain gauge observed precipitation, and re-optimized with WRF QPF. With model
119 parameter re-optimization, the model's performance improved, model parameters
120 should be optimized with QPF, not the rain gauge precipitation. Flood forecasting
121 products produced by coupling Liuxihe Model with WRF QPF provides good
122 reference for large watershed flood warning due to its long lead time and rational
123 results.



124 **2 Studied area and data**

125 2.1 Studied area

126 Liujiang River Basin(LRB) is selected as the studied area, which is the largest first
127 order tributary of the Pearl River with a drainage area of 58270 km²(Chen et. al.,
128 2016). LRB is in the monsoon area with heavy storms that induces severe flooding in
129 the watershed, and caused huge flood damages in the past centuries. Fig. 1 is a sketch
130 map of LRB.

131

132 Fig. 1 is here

133

134 2.2 Rain gauge precipitation and river flow discharge

135 Precipitation of 68 rain gauges within the watershed in 2011, 2012 and 2013 was
136 collected and used in this study to compare with the WRF QPF. Precipitation data is at
137 one hour interval. River discharge near the watershed outlet is collected also for this
138 same period. As this study focus on watershed flood forecasting, so only the
139 precipitation and river discharge during the flood events are prepared. There is one
140 flood event in each year, the flood events are numbered as flood event 2011, flood
141 event 2012 and flood event 2013 respectively.

142 **3 WRF QPF and post-processing**

143 3.1 WRF model

144 The WRF model (Skamarock et. al., 2005, 2008) is considered as the next
145 generation's medium term weather forecasting model, and can simulate different



146 weather processes from cloud scale to synoptic scale, especially in horizontal
147 resolution of 1 ~ 10 km. Also, it integrates the advanced numerical methods and data
148 assimilation techniques, a variety of physically process schemes, and multiple nested
149 methods and the capability of being used in different geographical locations. The
150 development of WRF model satisfies the needs of scientific research and practical
151 application, and could be further improved and strengthened. Now WRF model has
152 replaced the previously used MM5 model.

153

154 Many studies have been carried out in quantitative precipitation forecasting by using
155 WRF model, for example, Kumar et al. (2008) used WRF model to study a heavy rain
156 in 2005, the result showed that WRF system could reproduce the storm event and its
157 dynamical and thermo-dynamical characteristics. Hong and Lee (2009) set up a triply
158 nested WRF model to simulate the initiation of a thunderstorm, conducted the
159 sensitivity test. Maussion et. al. (2011) compared the capability of WRF model in
160 retrieving monthly precipitation and snowfall at three different spatial resolution
161 including 30、10 and 2 km, the result showed that WRF model had a good
162 performance in simulating monthly precipitation and snowfall in Tibet. Givati et al.
163 (2012) predicted the hiemal precipitation event of 2008 and 2009 based on WRF
164 model in upstream of the Jordan River, and coupled WRF model with hydrological
165 model-HYMKE to simulate the velocity and discharge of Jordan River. Pennelly et. al.
166 (2014) employed WRF model to predict three precipitation events of Alberta,
167 Canada, and compared the precipitation with 48 hour leading time predicted by WRF
168 model and the precipitation observed by rain gauges, the result showed that
169 Kain-Fritsch scheme overestimated the value of precipitation invariably. Zhang (2004)



170 introduced the WRF version 2 and grapes 3d variation assimilation, the simulation
171 and real-time forecasting results of weather conditions showed that WRF model had a
172 good performance in forecasting all kinds of weather conditions and had the ability to
173 predict the air quality. Niu et. al. (2007) tested the sensitivity of microphysical scheme
174 to a typical heavy rain based on WRF model, and analyzed the performance of
175 precipitation predicted from the precipitation region, center position and rainfall
176 intensity. Xu et. al. (2007) compared the hiemal continuous precipitation process
177 predicted with the estival results by WRF model, the results showed that the KF
178 scheme was better than BM scheme in summer. Hu et. al. (2008) found that the
179 parameterization scheme of WRF model was related to the model resolution, and the
180 parameterization scheme should be selected by the resolution of WRF model.
181 Huang et. al. (2011) found that variations in the microphysical process
182 parameterization schemes had much more influence on precipitation than that of
183 cumulus parameterization schemes, especially for a torrential rain attributed to
184 large-scale forcing that mainly resulted from stratus clouds. Wang and Ma (2011)
185 introduced the application of WRF model from the physics parameterization scheme,
186 real-time simulation study and the comparison with MM5 model in China in recent
187 decade. Pan et. al. (2012) used two WRF simulation groups between pre-process and
188 post-process in Heihe river basin, and compared and analyzed the mean bias error,
189 root mean square error and correlation coefficient of the two WRF groups.

190 3.2 WRF QPE of LRB

191 The WRF model (version 3) was set up in LRB by Li et. al. (2014), the model domain
192 is centered at 23.8N, 109.2W, and the projection is Lambert conformal projection. The
193 vertical structure includes 28 layers covering the whole troposphere. The WRF



194 single-moment 3-class microphysics parameterization, i.e., the Kain-Fritsch (Kain,
195 2004) and cumulus parameterization (Hong and Lim, 2006) were adopted for
196 precipitation simulation. The parameterization scheme of WRF is more than that of
197 other mesoscale numerical weather prediction (NWP), which includes 5 kinds of
198 physical parameterization schemes: microphysical process, cumulus, land surface
199 processes, atmospheric radiation and planetary boundary layer. There are 13
200 microphysical process parameterization schemes, Purdue Lin scheme was used in this
201 study as microphysical process. The parameterization scheme of precipitation was
202 improved based on the scheme Lin et al. (1983) as well as Rutledge and Hobbs (1983),
203 which is more mature than other schemes and is suited to simulate the high resolution
204 real time data.

205

206 The spatial and temporal resolution of WRF is at 20km*20km and 1 hour respectively,
207 so there are 156 WRF grids in LRB. QPF products in 2011, 2012 and 2013 were
208 produced at 3 different lead time, respectively 24 hours, 48 hours and 72 hours. Fig. 2,
209 3 and 4 are WRF QPF in three different years, while (a) is the rain gauge precipitation,
210 (b) is the WRF QPF with 24 hour lead time, (c) is the WRF QPF with 48 hour lead
211 time, and (d) is the WRF QPF with 72 hour lead time.

212

213 Fig. 2 is here

214 Fig. 3 is here

215 Fig. 4 is here

216



217 3.3 Comparison of WRF QPF and rain gauges precipitation

218 WRF QPF and rain gauge precipitation are compared in this study. From the results of
219 Fig. 2, 3 and 4, it could be found that the temporal precipitation pattern of both
220 products are similar, there are some kinds of differences, but the difference is not
221 significant. To make further comparison, the accumulated precipitation of the three
222 flood events averaged over the watershed are calculated and listed in Table 1.

223

224 Table 1 is here

225

226 From the results of Table 1, it could be found that the WRF QPF accumulated
227 precipitation has obvious bias with rain gauge accumulated precipitation. For all the
228 three flood events, the WRF QPF accumulated precipitation are higher than those
229 estimated by rain gauge, i. e., the WRF QPF overestimates the precipitation. For flood
230 event 2011, the overestimated watershed averaged precipitation of WRF QPF with
231 lead time of 24 hour, 48 hour and 72 hour are 23%, 32% and 55% respectively, for
232 flood event 2012, they are 16%, 37% and 71% respectively, for flood event 2013, they
233 are 50%, 73% and 95% respectively. This also means that the longer the WRF QPF
234 lead time, the higher the overestimation.

235 3.4 WRF QPF post-processing

236 From the results of Fig. 2, 3 and 4, and Table 1, the WRF QPF has significant bias
237 with rain gauge precipitation. If the rain gauge precipitation is assumed correct, then
238 WRF QPF has error. So in this study the WRF QPF is post-processed based on the
239 rain gauge precipitation to correct the systematic error of WRF QPF. The principle of



240 WRF QPF post-processing proposed in this study is to keep the areal averaged event
241 accumulated precipitation from both products are similar, i.e., to adjust the WRF QPF
242 precipitation to make its event accumulated precipitation equal to that of rain gauge.
243 Based on this principle, the WRF QPF post-processing procedure is summarized as
244 follows:

245

246 1) Calculate the areal average precipitation of the WRF QPF for each flood events
247 over the watershed as following equation.

$$248 \quad \bar{P}_{WRF} = \frac{\sum_{i=1}^N P_i F_i}{N} \quad (1)$$

249 Where, \bar{P}_{WRF} is the areal average precipitation of WRF QPF of one flood event, P_i is
250 the precipitation on WRF grid i , F_i is the drainage area of WRF grid i , N is the total
251 number of WRF grids.

252 2) Calculate the areal average precipitation of the rain gauges with the following
253 equation.

$$254 \quad \bar{P}_2 = \frac{\sum_{j=1}^M P_j}{M} \quad (2)$$

255 Where, \bar{P}_2 is the areal average precipitation of the rain gauges network, P_j is the
256 precipitation observed by j th rain gauge, M is the total number of rain gauges.

257 3) The precipitation of every WRF QPF grids then could be revised with the



258 following equation.

$$259 \quad P'_i = P_i \frac{\bar{P}_2}{\bar{P}_{WRF}} \quad (3)$$

260 Where, P'_i is the revised precipitation of ith WRF grid.

261 With the above WRF QPF post-processing method, the WRF QPF of flood event 2011,
262 2012 and 2013 were post-processed, and will be used to couple with the Liuxihe
263 Model for flood simulation.

264 **3 Hydrological model**

265 **3.1 Liuxihe Model**

266 Liuxihe model is a physically based fully distributed hydrological model proposed
267 mainly for watershed flood forecasting (Chen, 2009, Chen et. al., 2011), and has been
268 used in a few watersheds flood forecasting(Chen, 2009, Chen et. al., 2011, 2013, 2016,
269 Liao et. al., 2012 a, b, Xu et. al., 2012 a, b). In Liuxihe Model, runoff components are
270 calculated at grid scale, runoff routes at both grid and watershed scale. Runoff routing
271 is divided into hill slope routing and river channel routing by using different
272 computation algorithm. Liuxihe Model proposed an automatic parameter optimization
273 method using PSO algorithm (Chen et. al., 2016), which largely improves the model's
274 performance in watershed flood forecasting. Now Liuxihe Model is deployed on a
275 supercomputer system with parallel computation techniques (Chen et. al., 2013) that
276 largely facilitates the model parameter optimization of Liuxihe Model.

277

278 Chen et. al. (2016) set up Liuxihe Model in LRB with freely downloaded terrain
279 property data from the website at a spatial resolution of 200m*200m, and optimized
280 model parameters with observed hydrological data. The model was validated by



281 observed flood events data, and the model performance is found rational and could be
282 used for real-time flood forecasting. The model only uses rain gauge precipitation, so
283 its flood forecasting lead time is limited. In this study, the Liuxihe Model set up in
284 LRB and the optimized model parameters will be used in this study as the first
285 attempt, Fig. 5 is the model structure.

286

287 Fig.5 is here

288

289 3.2 Liuxihe Model parameter optimization

290 As the model parameters optimized by Chen et. al. (2016) is done by using the rain
291 gauge precipitation, but this study uses the WRF QPF as the precipitation input, so the
292 parameters of Liuxihe Model set up in LRB may not appropriate for coupling the
293 WRF QPF. For this reason, considering Liuxihe Model is a physically based
294 distributed hydrological model, one flood event could be used for parameter
295 optimization, the parameters were optimized again by using the WRF QPF in 2011,
296 the WRF QPF is the post-processed one, not the original one. Results of parameter
297 optimization are shown in Fig. 6, among them, (a) is the objective function evolution
298 result, (b) is the parameters evolution result, and (c) is the simulated flood process by
299 using the optimized model parameters. To compare, the simulated flood process of
300 flood event 2011 was also drawn in Fig. 6(c).

301

302 Fig. 6 is here

303

304 From the result of Fig. 6(c), it could be found that the optimized model parameters



305 with WRF QPF improved much than that simulated with rain gauge precipitation, this
306 means parameter optimization with WRF QPF is necessary.

307 3.3 Coupling WRF QPF with Liuxihe Model for LRB flood forecasting

308 The Liuxihe Model set up for LRB flood forecasting (Chen et. al., 2016) is employed
309 to couple with the WRF QPF, the model spatial resolution remains to be 200m*200m.
310 As the spatial resolution of WRF QPF is at 20km*20km, the WRF QPF was
311 downscaled to the resolution of 200m*200m by using the nearest downscaling
312 method, the same spatial resolution of the flood forecasting model.

313 4 Results and discussions

314 4.1 Effects of WRF post-processing

315 The original WRF QPF and the post-processed QPF are used to couple with the
316 Liuxihe Model, in this simulation, the original model parameters that is optimized
317 with the rain gauge precipitation are employed, not the re-optimized model
318 parameters, the simulated results are shown in Fig. 7, 8 and 9.

319

320 Fig. 7 is here

321 Fig. 8 is here

322 Fig. 9 is here

323

324 From the above results, it could be seen that the simulated flood discharges with the
325 original WRF QPF is much lower than the observed ones, but with post-processed
326 WRF QPF used, the simulated flood discharge increased and much more close to the



327 observation, this implies that the flood forecasting capability has been improved by
328 post-processing of WRF QPF. To further compare the three results, 5 evaluation
329 indices, including Nash-Sutcliffe coefficient(C), correlation coefficient(R), process
330 relative error(P), peak flow relative error(E) and water balance coefficient(W) are
331 calculated and listed in Table 2.

332

333 Table 2 is here

334

335 From the results of Table 2, it has been found that all the 5 evaluation indices have
336 been improved by coupling the post-processed WRF QPF. For example, to flood
337 event 2011 with 24 hour lead time, the Nash-Sutcliffe coefficient/C, correlation
338 coefficient/R, process relative error/P, peak flow relative error/E and coefficient of
339 water balance/W with original WRF QPF are 0.65, 0.88, 35%, 14% and 1.44
340 respectively, but those with the post-processed WRF QPF are 0.75, 0.93, 23%, 8%
341 and 1.15 respectively. To flood event 2012 with 48 hour lead time, the above 5
342 evaluation indices with original WRF QPF are 0.63, 0.75, 48%, 12% and 1.43
343 respectively, and are 0.75, 0.84, 26%, 8% and 1.32 respectively with the
344 post-processed WRF QPF. To flood event 2013 with 72 hour lead time, the above 5
345 evaluation indices with original WRF QPF are 0.44, 0.75, 129%, 45% and 1.66
346 respectively, and are 0.55, 0.82, 98%, 23%, 1.25 respectively with the post-processed
347 WRF QPF. It is obvious that with the post-processed WRF QPF, the evaluation
348 indices are improved much more. These results show that WRF QPF post processing
349 could improve the flood forecasting capability because the WRF QPF is more close
350 to the observed precipitation after post-processing, so it should be done for real-time
351 flood forecasting.



352 4.2 Results comparison for different model parameters

353 The model parameters optimized with rain gauge precipitation and WRF QPF are
354 different, so different parameter will have different model performance. To analyze
355 this effect, the flood events of 2012 and 2013 with two different sets of model
356 parameters are simulated, and are shown in Fig. 10 and Fig. 11 respectively, only the
357 post-processed WRF QPF are coupled in this simulation.

358

359 Fig. 10 is here

360 Fig. 11 is here

361

362 From the above results it has been found that the simulated flood results with
363 re-optimized model parameters is better than that simulated with the original model
364 parameters, the simulated flood discharge with the re-optimized model parameters is
365 more fitting the observation. To further compare the two results, 5 evaluation indices,
366 including Nash-Sutcliffe coefficient(C), correlation coefficient(R), process relative
367 error(P), peak flow relative error(E) and water balance coefficient(W) are calculated
368 and listed in Table 3.

369

370 Table 3 is here

371

372 From the results of Table 3, it has been found that the results of flood simulation
373 based on the re-optimized model parameters have better evaluation indices. All
374 evaluation indices for that based on re-optimized model parameters improved. For
375 example, for flood event 2012 with 24 hour lead time, the Nash-Sutcliffe



376 coefficient/C, correlation coefficient/R, process relative error/P, peak flow relative
377 error/E and coefficient of water balance/W with original model parameters are 0.58,
378 0.82, 35%, 12% and 1.08 respectively, but those with the re-optimized model
379 parameters are 0.74, 0.86, 28%, 8% and 0.95 respectively. For flood event 2013 with
380 48 hour lead time, the 5 indices with the original model parameters are 0.62, 0.86,
381 22%, 13% and 1.24 respectively, and are 0.68, 0.89, 18%, 9% and 1.06 respectively
382 for those with re-optimized model parameters. So it could be said that in coupling the
383 WRF QPF with distributed hydrological model, the model parameters needs to be
384 re-optimized with the WRF QPF. This finding implies that the precipitation pattern
385 has obvious impact to model parameters, it should be considered, and model
386 parameter optimization is a rational way for considering this effect.

387

388 4.3 Flood simulation accuracy with different lead time

389 To compare the model performance with different lead time, the flood events with 3
390 different lead time is simulated and shown in Fig. 12, the model parameters are the
391 re-optimized ones, and the QPF is the post-processed QPF.

392

393 Fig. 12 is here

394

395 From the results of Fig. 12, it could be seen that the flood simulation result gets worse
396 as the lead time increases, i.e., the model performance with 24 hour lead time is better
397 than that with 48 hour lead time, and the model performance with 48 hour lead time is
398 better than that with 72 hour lead time. The simulated hydrological process with 24
399 hour lead time is very similar with that simulated with rain gauge precipitation. To
400 further compare the results, 5 evaluation indices, including Nash-Sutcliffe



401 coefficient(C), correlation coefficient(R), process relative error(P), peak flow relative
402 error(E) and water balance coefficient(W) are calculated and listed in Table 4.

403

404 Table 4 is here

405

406 From the results of Table 4, it has been found that the simulated flood events with 24
407 hour lead time has best evaluation indices, and is very close to that simulated with
408 rain gauge precipitation. For flood event 2012, the Nash-Sutcliffe coefficient/C,
409 correlation coefficient/R, process relative error/P, peak flow relative error/E and
410 coefficient of water balance/W with rain gauge are 0.82, 0.89, 20%, 5% and 0.8
411 respectively, those with 24 hour lead time are 0.74, 0.86, 28%, 8% and 0.95
412 respectively, those with 48 hour lead time are 0.63, 0.84, 48%, 12% and 1.32
413 respectively, and are 0.56, 0.56, 56%, 18% and 1.54 respectively for 72 hour lead time.
414 For flood event 2013, the Nash-Sutcliffe coefficient/C, correlation coefficient/R,
415 process relative error/P, peak flow relative error/E and coefficient of water balance/W
416 with rain gauge are 0.95, 0.92, 8%, 6% and 1.08 respectively, those with 24 hour lead
417 time are 0.87, 0.87, 9%, 12% and 1.02 respectively, those with 48 hour lead time are
418 0.62, 0.86, 22%, 13% and 1.24 respectively, and are 0.61, 0.87, 75%, 17% and 1.66
419 respectively for 72 hour lead time. This finding means that the current WRF QPF
420 capability is lead-time dependent, and with the increasing of lead time, the practical
421 value of WRF QPF gets lower.

422 **5 Conclusion**

423 In this study, the WRF QPF is coupled with a distributed hydrological model-the
424 Liuxihe model for large watershed flood forecasting, and three lead time of WRF QPF



425 products, including 24 hours, 48 hours and 72 hours are tested. WRF QPF post
426 processing method is proposed and tested, model parameters are re-optimized by
427 using the post-processed WRF QPF, model performance are compared among very
428 conditions. Based on the results of this study, the following conclusions could be
429 drawn:

430

431 1) The quantitative precipitation forecasting produced by WRF model has a similar
432 pattern with that estimated by rain gauges temporally, but overestimated the averaged
433 watershed precipitation on the event accumulated total precipitation, and the longer
434 the WRF QPF lead time, the higher the precipitation overestimation. For flood event
435 2011, the overestimated watershed averaged precipitation of WRF QPF with lead time
436 of 24 hour, 48 hour and 72 hour are 23%, 32% and 55% respectively, for flood event
437 2012, these are 16%, 37% and 71% respectively, while for flood event 2013, these are
438 50%, 73% and 95% respectively.

439

440 2. WRF QPF has systematic bias compared with rain gauge precipitation, and this
441 bias could be reduced via post-processing. Principle used in this study for WRF QPF
442 post processing is effective and could improve the flood forecasting capability. For
443 flood event 2011 with 24 hour lead time, the Nash-Sutcliffe coefficient/C, correlation
444 coefficient/R, process relative error/P, peak flow relative error/E and coefficient of
445 water balance/W with original WRF QPF are 0.65, 0.88, 35%, 14% and 1.44
446 respectively, but those with the post-processed WRF QPF are 0.75, 0.93, 23%, 8%
447 and 1.15 respectively. For flood event 2012 with 48 hour lead time, the above 5
448 evaluation indices with original WRF QPF are 0.63, 0.75, 48%, 12% and 1.43
449 respectively, and are 0.75, 0.84, 26%, 8% and 1.32 respectively with the



450 post-processed WRF QPF. For flood event 2013 with 72 hour lead time, the above 5
451 evaluation indices with original WRF QPF are 0.44, 0.75, 129%, 45% and 1.66
452 respectively, and are 0.55, 0.82, 98%, 23%, 1.25 respectively with the post-processed
453 WRF QPF.

454

455 3. Hydrological model parameters optimized with the rain gauge precipitation needs
456 to be re-optimized using the post-processed WRF QPF, this improves the model
457 performance largely, i.e., in coupling distributed hydrological model with QPF for
458 flood forecasting, the model parameters should be optimized with the QPF produced
459 by WRF. For flood event 2012 with 24 hour lead time, the Nash-Sutcliffe
460 coefficient/C, correlation coefficient/R, process relative error/P, peak flow relative
461 error/E and coefficient of water balance/W with original model parameters are 0.58,
462 0.82, 35%, 12% and 1.08 respectively, but those with the re-optimized model
463 parameters are 0.74, 0.86, 28%, 8% and 0.95 respectively. For flood event 2013 with
464 48 hour lead time, the 5 indices with the original model parameters are 0.62, 0.86,
465 22%, 13% and 1.24 respectively, and are 0.68, 0.89, 18%, 9% and 1.06 respectively
466 for those with re-optimized model parameters.

467

468 4. The simulated floods by coupling WRF QPF with distributed hydrological model is
469 rational and could benefit the flood management communities due to its longer lead
470 time for flood warning, it provides a good reference for large watershed flood warning.
471 But with the lead time getting longer, the flood forecasting accuracy is getting lower.
472 For flood event 2012, the Nash-Sutcliffe coefficient/C, correlation coefficient/R,
473 process relative error/P, peak flow relative error/E and coefficient of water balance/W
474 with rain gauge are 0.82, 0.89, 20%, 5% and 0.8 respectively, those with 24 hour lead



475 time are 0.74, 0.86, 28%, 8% and 0.95 respectively, those with 48 hour lead time are
476 0.63, 0.84, 48%, 12% and 1.32 respectively, and are 0.56, 0.56, 56%, 18% and 1.54
477 respectively for 72 hour lead time. For flood event 2013, the Nash-Sutcliffe
478 coefficient/C, correlation coefficient/R, process relative error/P, peak flow relative
479 error/E and coefficient of water balance/W with rain gauge are 0.95, 0.92, 8%, 6%
480 and 1.08 respectively, those with 24 hour lead time are 0.87, 0.87, 9%, 12% and 1.02
481 respectively, those with 48 hour lead time are 0.62, 0.86, 22%, 13% and 1.24
482 respectively, and are 0.61, 0.87, 75%, 17% and 1.66 respectively for 72 hour lead
483 time.

484 **Acknowledgements**

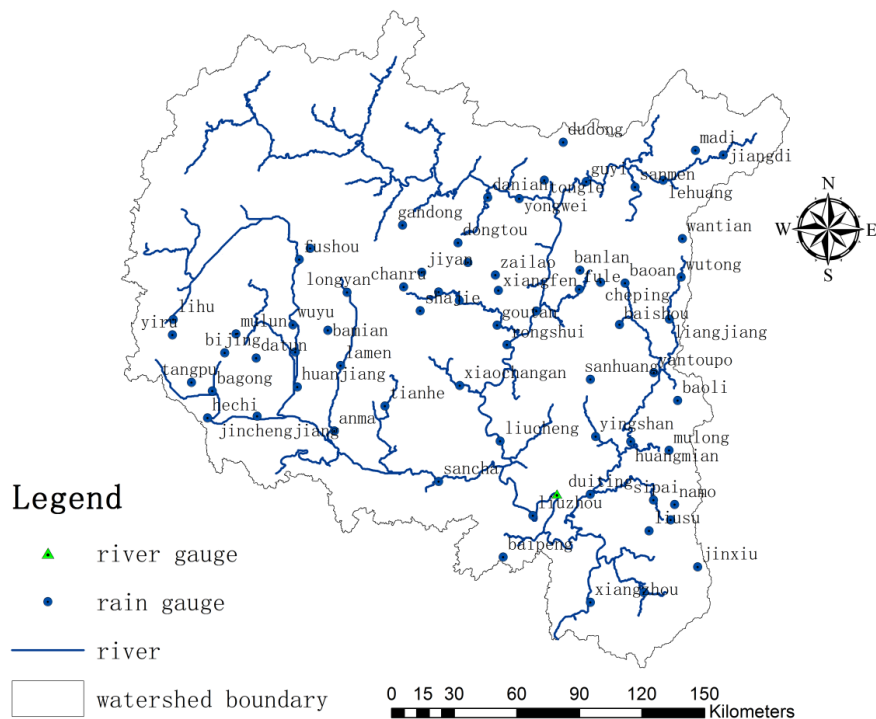
485 This study is supported by the Special Research Grant for the Water Resources
486 Industry (funding no. 201301070), the National Science Foundation of China (funding
487 no. 50479033), and the Basic Research Grant for Universities of the Ministry of
488 Education of China (fundingno.13lgjc01).

489



490

491 **Figures**



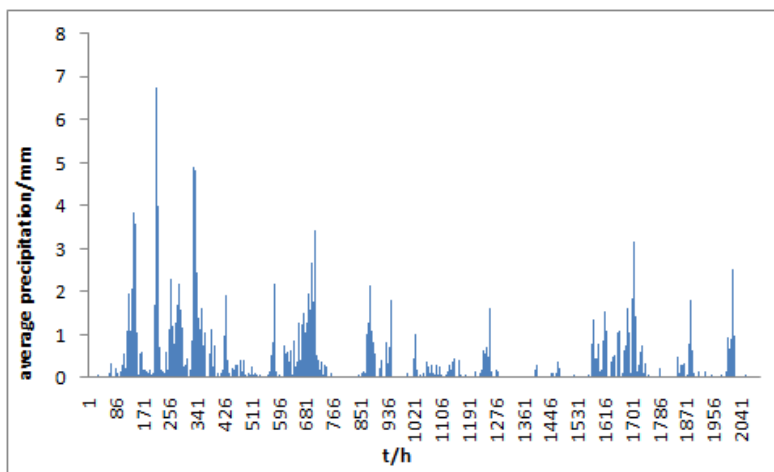
492

493

Fig. 1 Sketch map of Liujiang River Basin(Chen et. al., 2016)

494

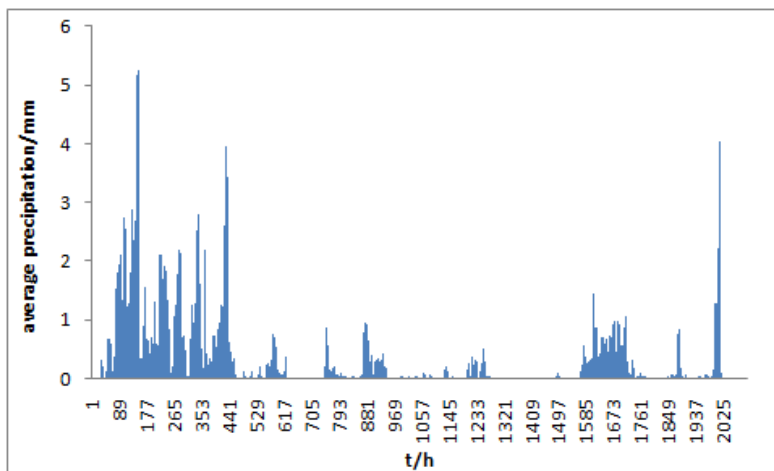
495



496

497

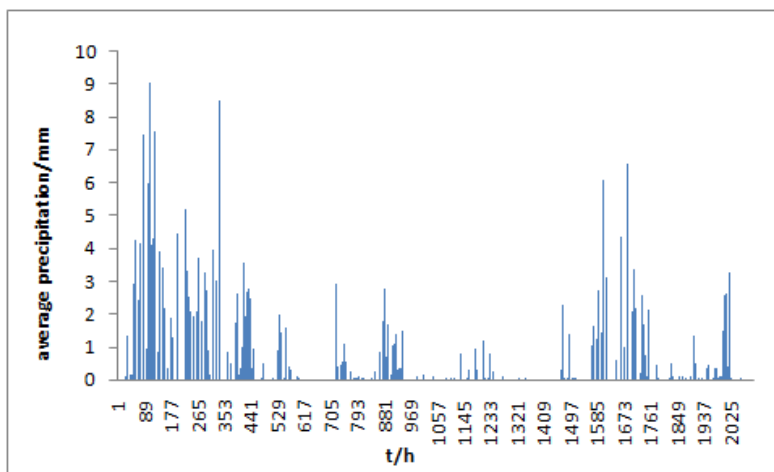
(a)



498

499

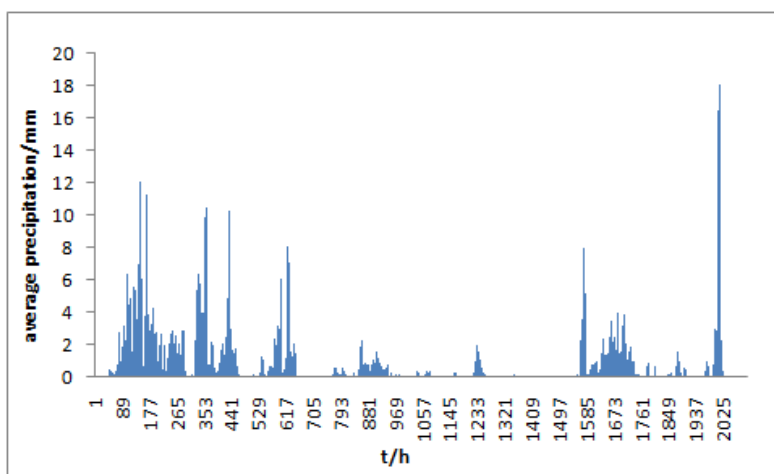
(b)



500

501

(c)



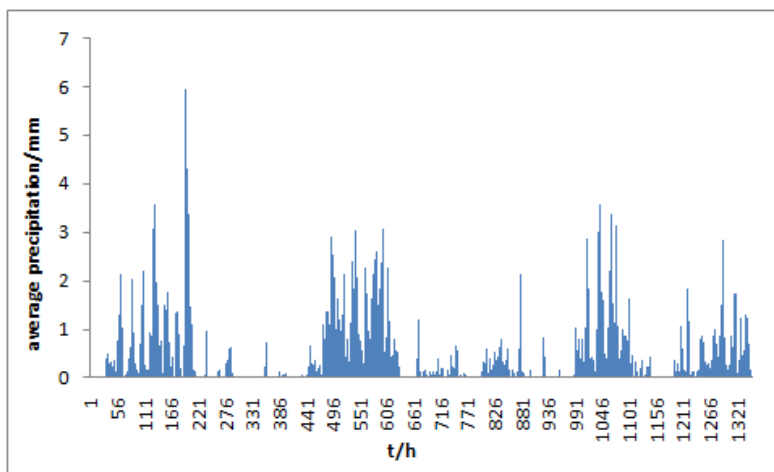
502

503

(d)

504 Fig. 2 Precipitation pattern comparison of two precipitation products(2011), (a) is the
505 average precipitation of rain gauges, (b) is the average precipitation of WRF with 24
506 hour lead time, (c) is the average precipitation of WRF with 48 hour lead time, (d) is
507 the average precipitation of WRF with 72 hour lead time.

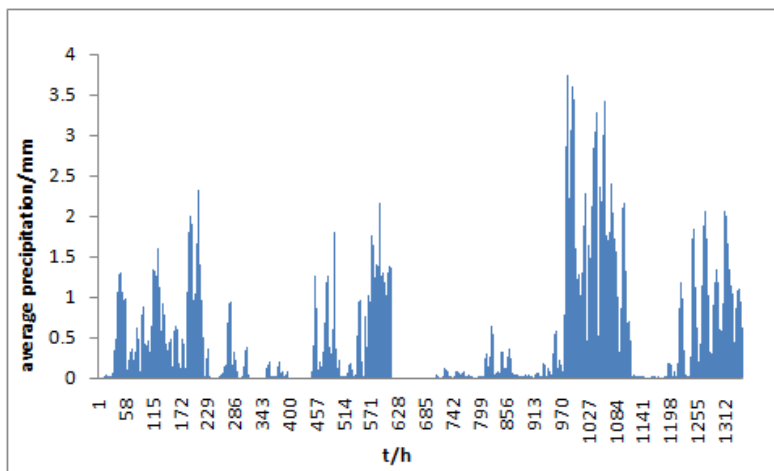
508



509

510

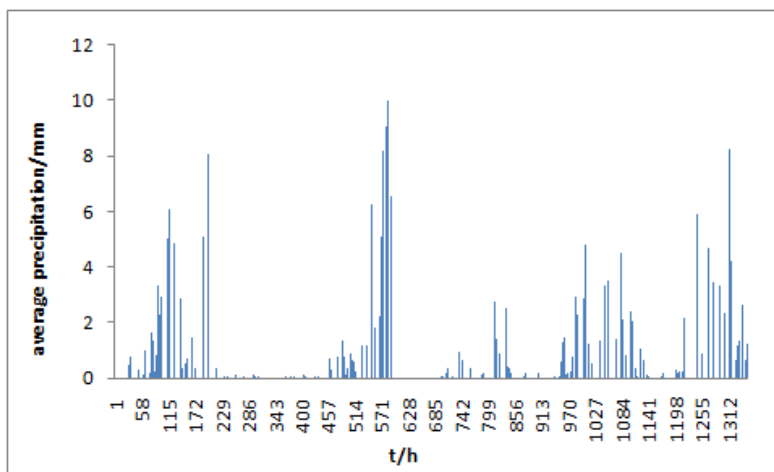
(a)



511

512

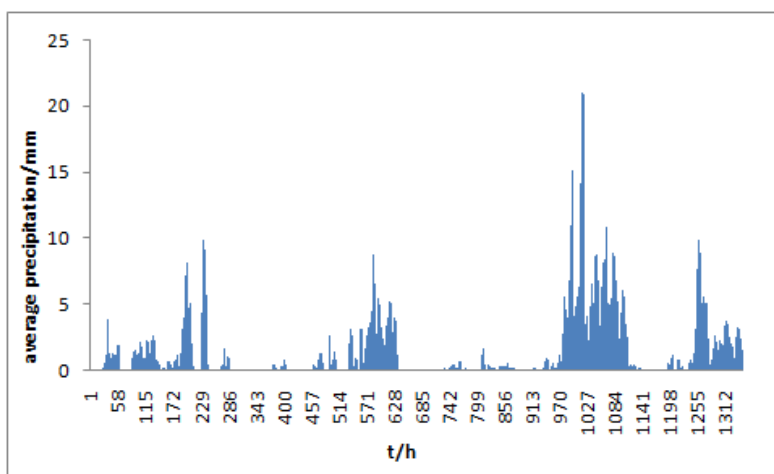
(b)



513

514

(c)



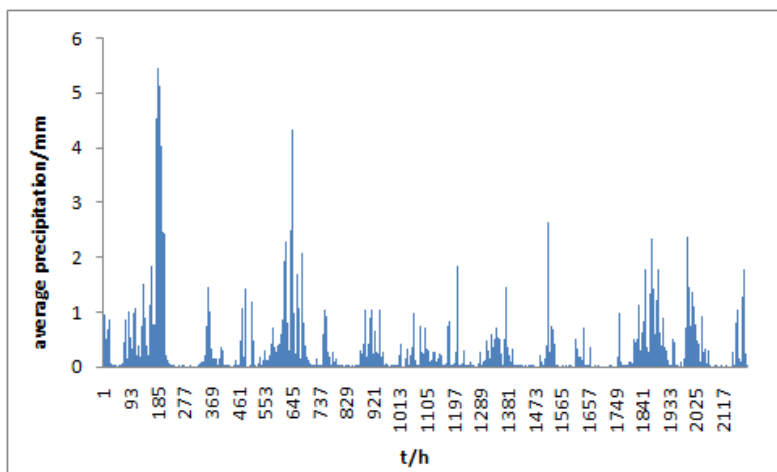
515

516

(d)

517 Fig. 3 Precipitation pattern comparison of two precipitation products(2012) , (a) is the
518 average precipitation of rain gauges, (b) is the average precipitation of WRF with 24
519 hour lead time, (c) is the average precipitation of WRF with 48 hour lead time, (d) is
520 the average precipitation of WRF with 72 hour lead time.

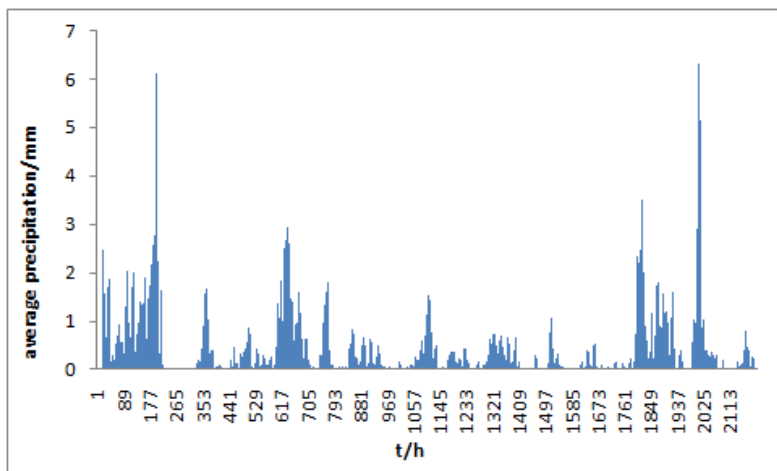
521



522

523

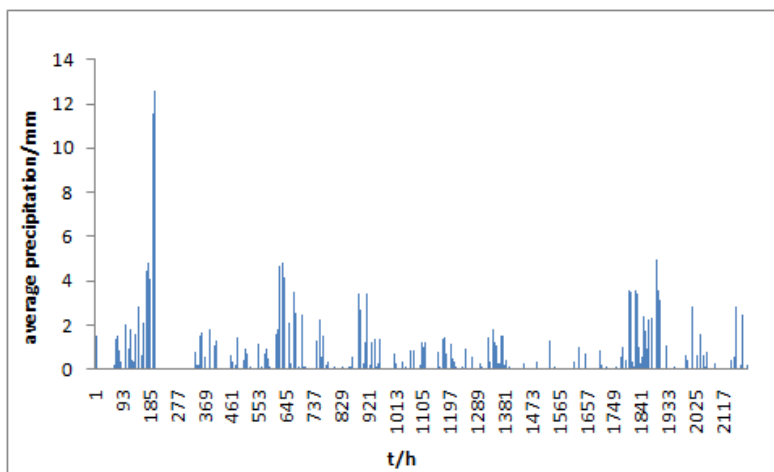
(a)



524

525

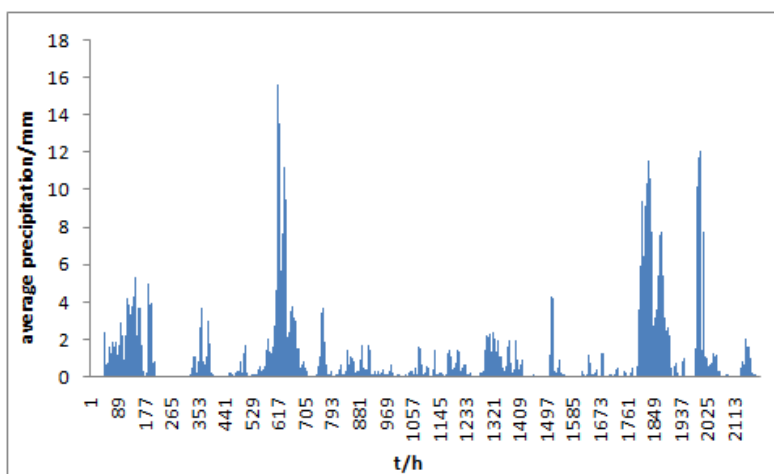
(b)



526

527

(c)

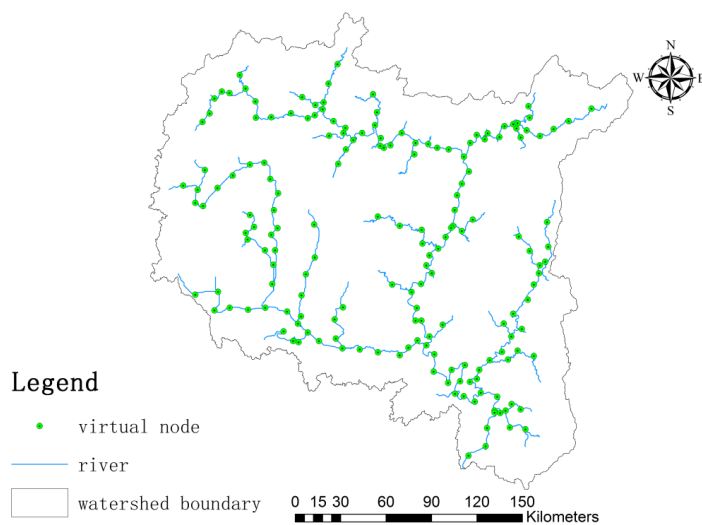


528

529

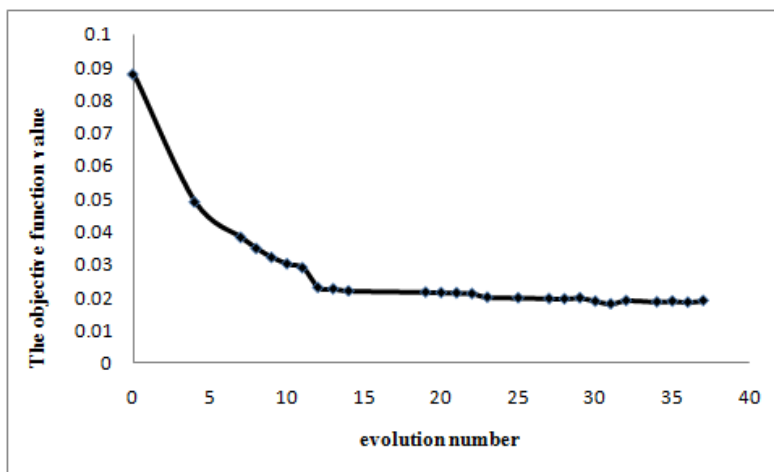
(d)

530 Fig. 4 Precipitation pattern comparison of two precipitation products(2013), (a) is the
531 average precipitation of rain gauges, (b) is the average precipitation of WRF with 24
532 hour lead time, (c) is the average precipitation of WRF with 48 hour lead time, (d) is
533 the average precipitation of WRF with 72 hour lead time.



534

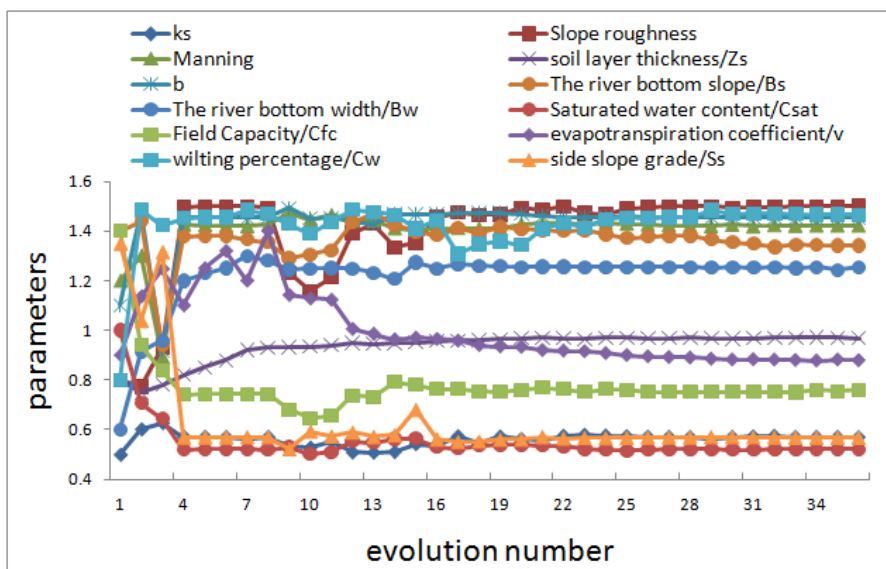
535 Fig.5 Liuxihe Model structure of LRB (200m×200m resolution, Chen et. al., 2016)



536

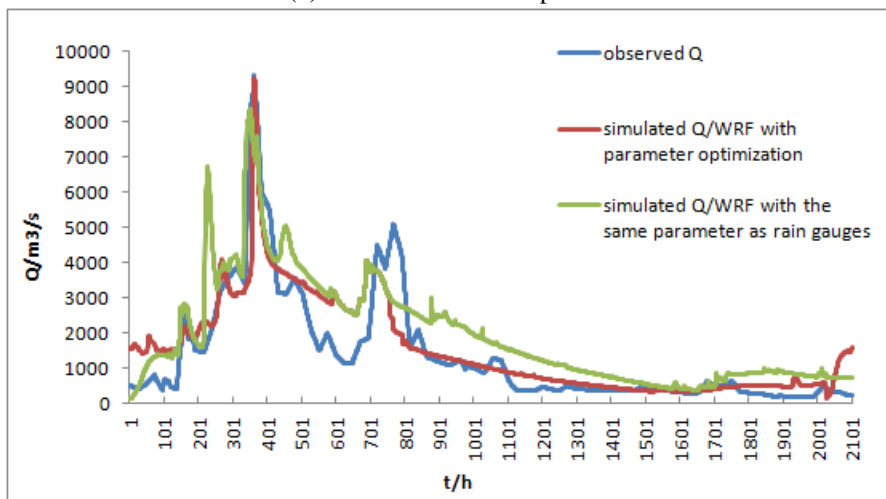
537

(a) Evolutionary process of objective function



538
 539

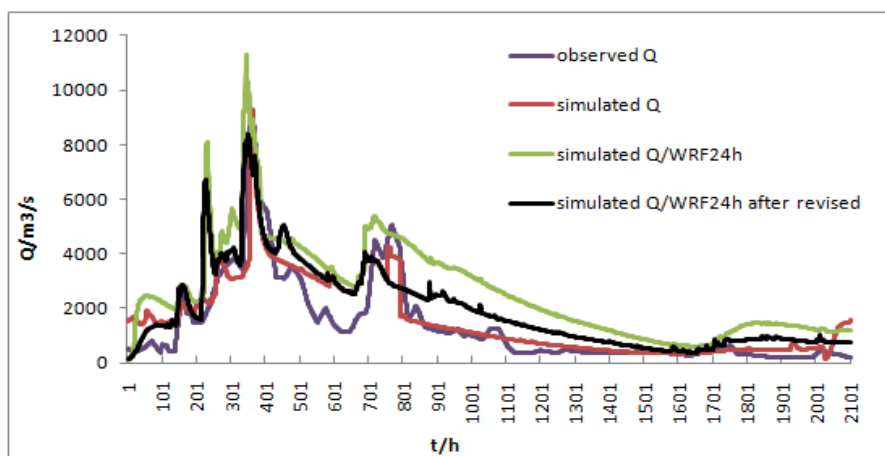
(b) Parameter evolution process



540
 541
 542
 543

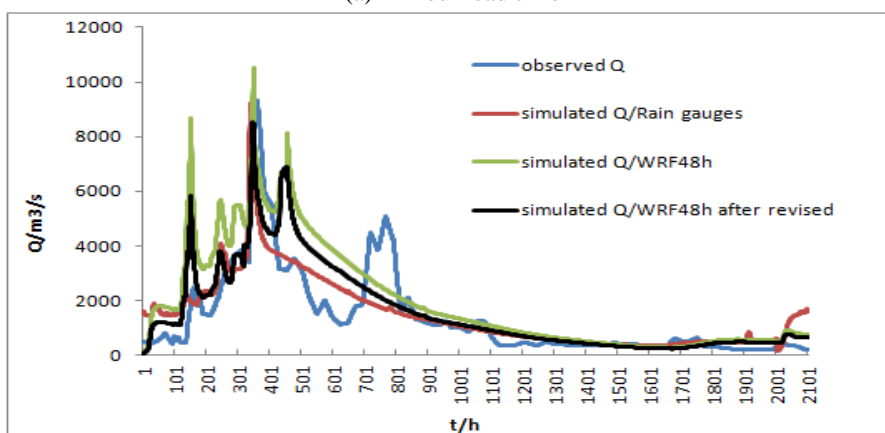
(c) Simulated flood process with optimized model parameters

Fig. 6 Parameter optimization results of Liuxihe Model for LRB with WRF QPF



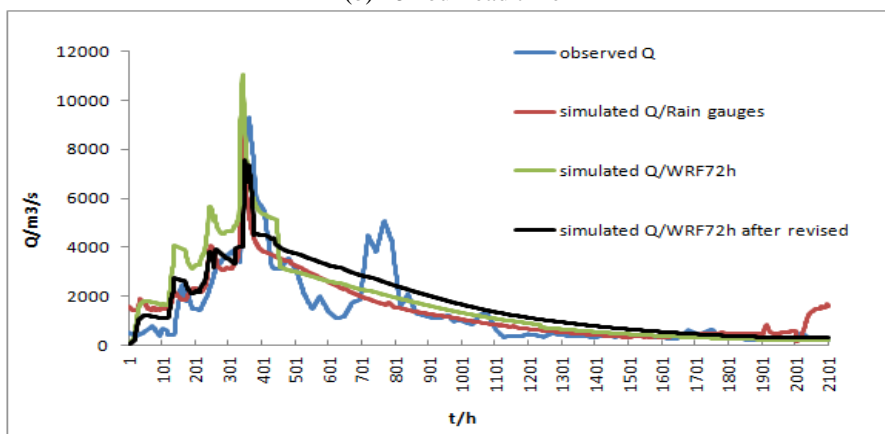
544
545

(a) 24 hour lead time



546
547

(b) 48 hour lead time



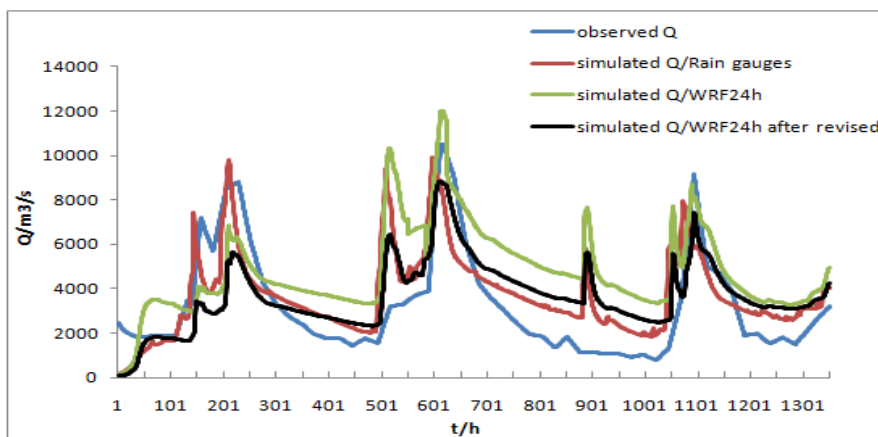
548
549
550

(c) 72 hour lead time

Fig. 7 Coupled flood simulation results with original model parameters (2011)

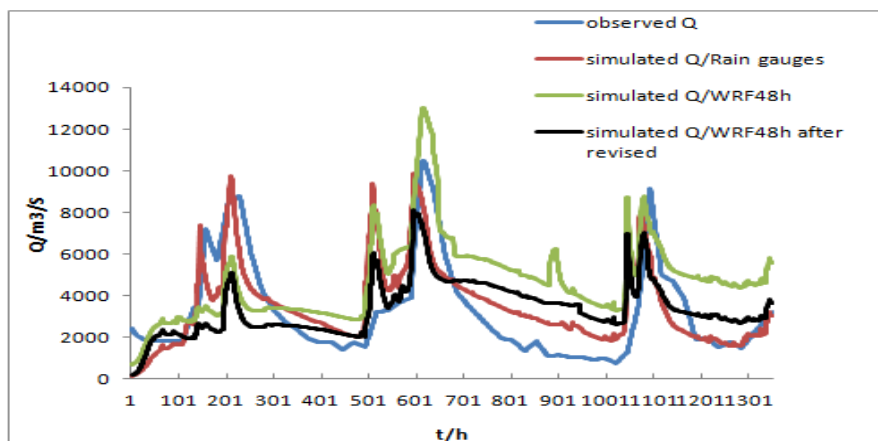


551
552



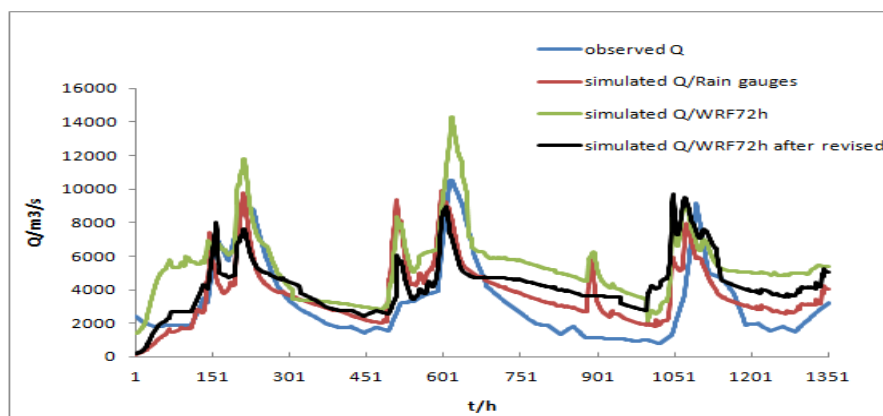
(a) 24 hour lead time

553
554



(b) 48 hour lead time

555
556
557

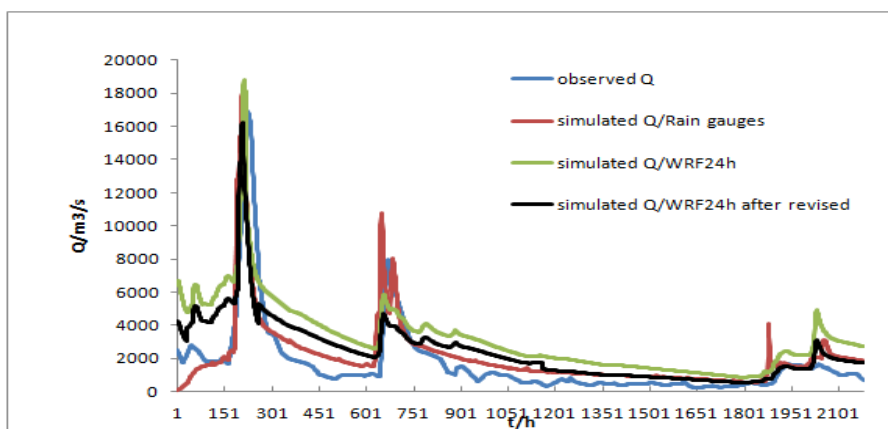


(c) 72 hour lead time

Fig. 8 Coupled flood simulation results with original model parameters(2012)

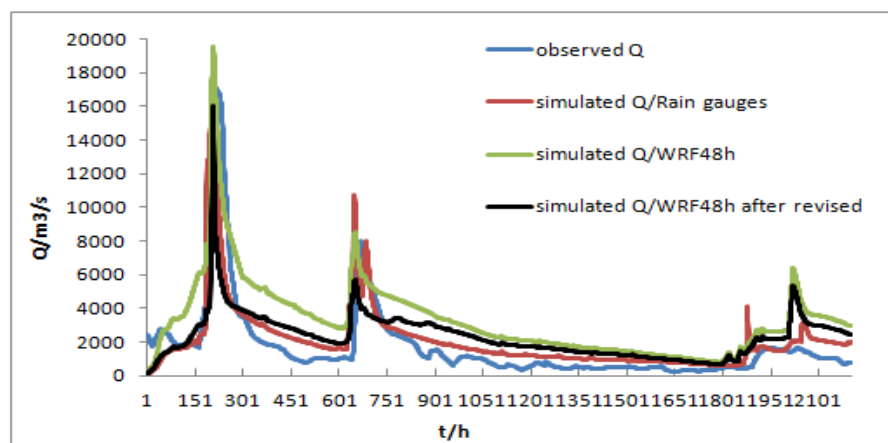


558
559



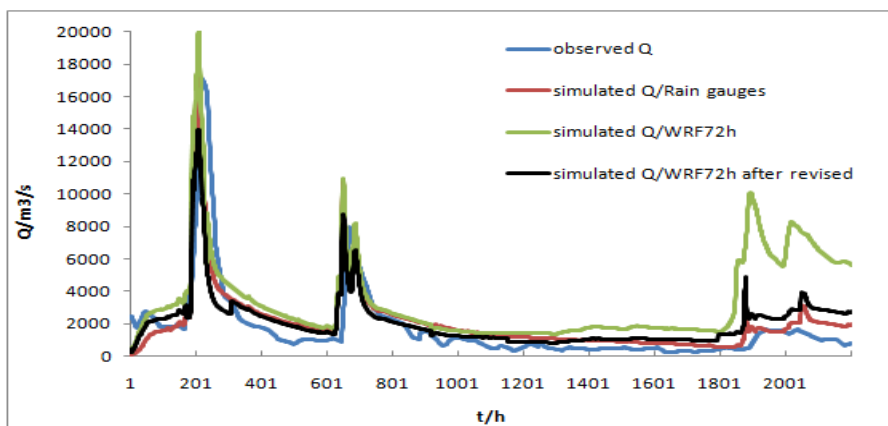
(a) 24 hour lead time

560
561



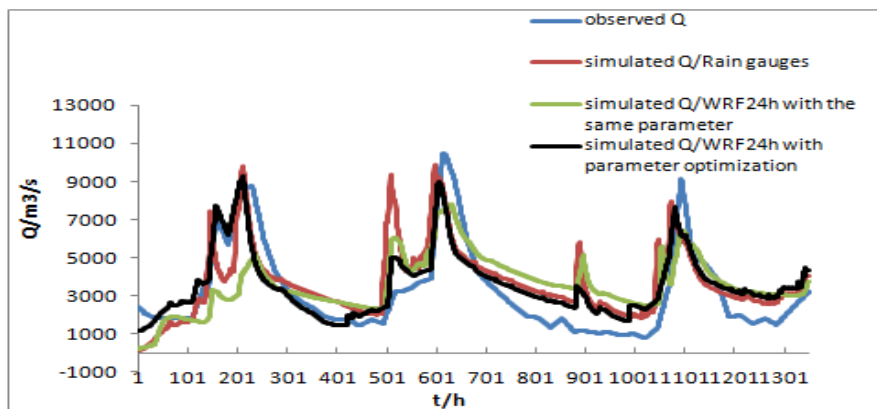
(b) 48 hour lead time

562
563
564



(c) 72 hour lead time

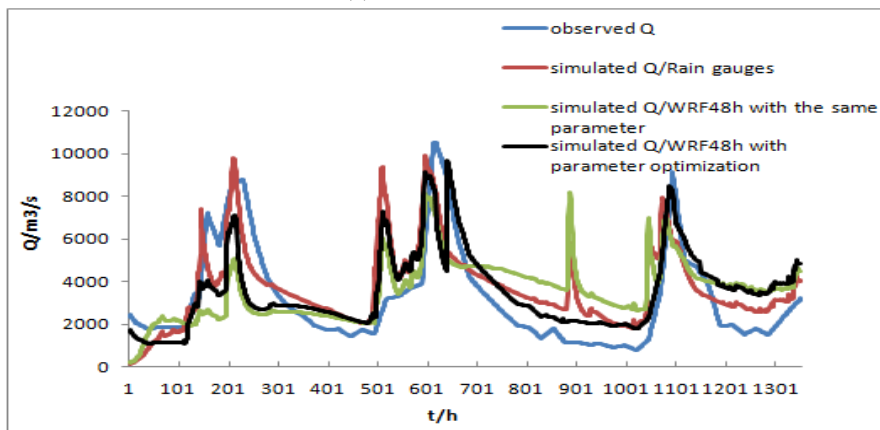
Fig. 9 Coupled flood simulation results with original model parameters (2013)



565

566

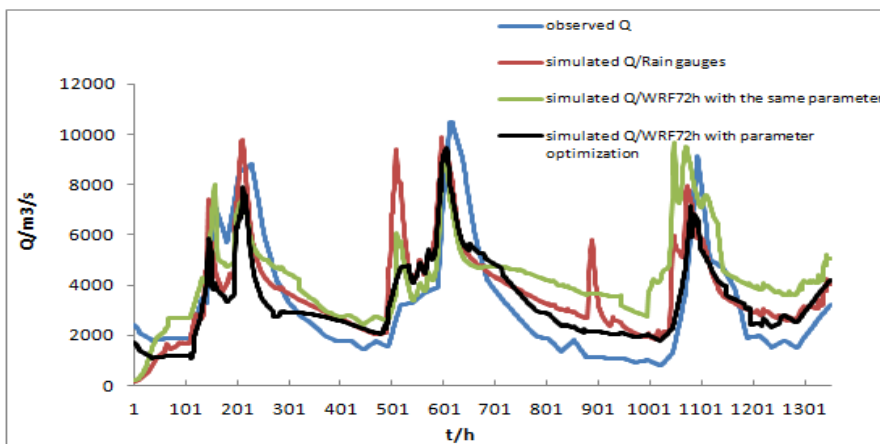
(a) 24 hour lead time



567

568

(b) 48 hour lead time



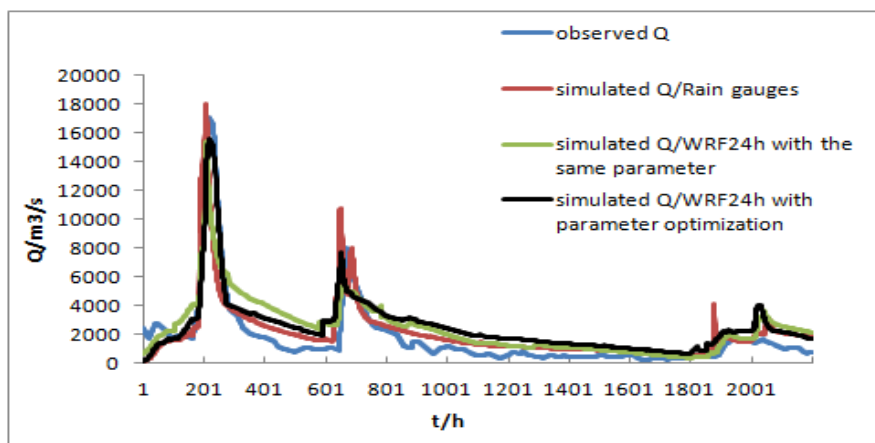
569

570

571

(c) 72 hour lead time

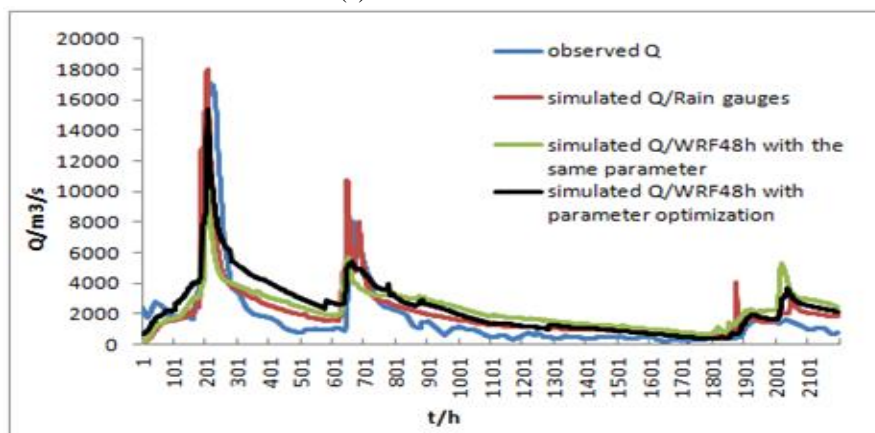
Fig. 10 Coupled flood simulation results with re-optimized model parameters (2012)



572

573

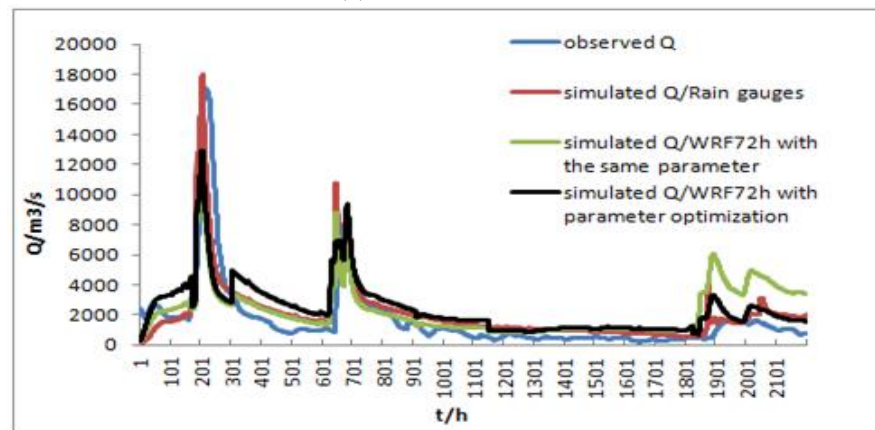
(a) 24 hour lead time



574

575

(b) 48 hour lead time



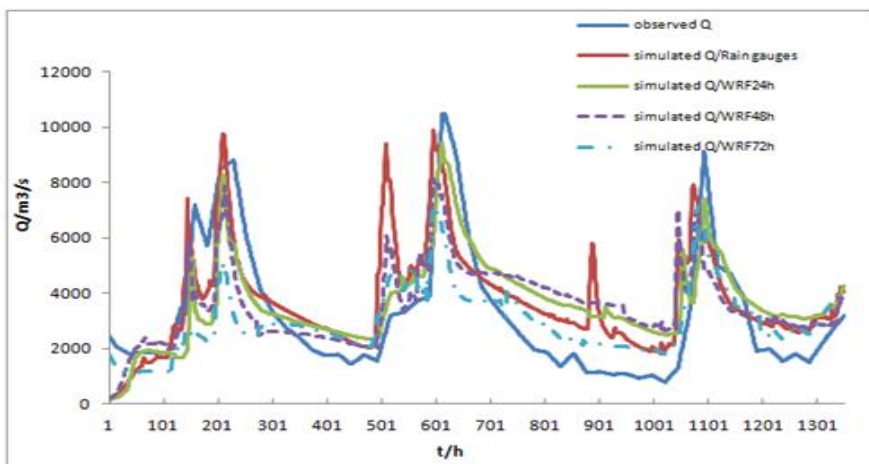
576

577

578

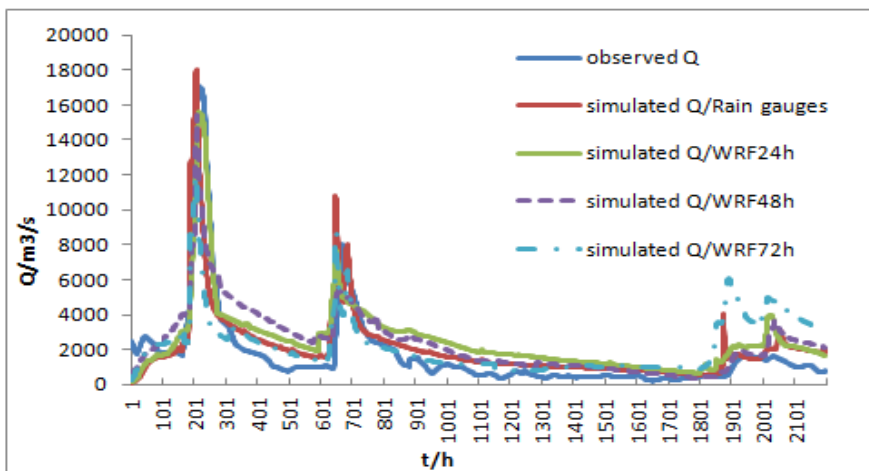
(c) 72 hour lead time

Fig. 11 Coupled flood simulation results with re-optimized model parameters (2013)



579
580

(a) Flood event 2012



581
582
583
584

(b) Flood event 2013

Fig. 12 Simulated results with different lead time



585 **Tables**

586 Table 1 Precipitation comparison of two products

Flood event no.	Precipitation products	average precipitation(mm)	relative bias %
2011	rain gauges	0.22	
	WRF/24h	0.27	23
	WRF/48h	0.29	32
	WRF/72h	0.34	55
2012	rain gauges	0.38	
	WRF/24h	0.44	16
	WRF/48h	0.52	37
	WRF/72h	0.65	71
2013	rain gauges	0.22	
	WRF/24h	0.33	50
	WRF/48h	0.38	73
	WRF/72h	0.43	95

587

588

589 Table 2 Evaluation indices of simulated flood events with post-processed WRF QPF

Rain type	statistical index	201101010	20120101	20130101
WRF/24h	Nash-Sutcliffe coefficient/C	0.65	0.48	0.65
	Correlation coefficient/R	0.88	0.73	0.83
	Process relative error/P	0.35	0.57	0.19
	Peak flow relative error/E	0.14	0.18	0.25
	The coefficient of water balance/W	1.44	1.35	1.38



WRF/24h after revised	Nash-Sutcliffe coefficient/C	0.75	0.58	0.75
	Correlation coefficient/R	0.93	0.82	0.85
	Process relative error/P	0.23	0.35	0.11
	Peak flow relative error/E	0.08	0.12	0.16
	The coefficient of water balance/W	1.15	1.08	1.12
WRF/48h	Nash-Sutcliffe coefficient/C	0.58	0.63	0.5
	Correlation coefficient/R	0.78	0.75	0.8
	Process relative error/P	0.52	0.48	0.34
	Peak flow relative error/E	0.41	0.12	0.24
	The coefficient of water balance/W	1.52	1.43	1.51
WRF/48h after revised	Nash-Sutcliffe coefficient/C	0.64	0.75	0.62
	Correlation coefficient/R	0.82	0.84	0.86
	Process relative error/P	0.45	0.26	0.22
	Peak flow relative error/E	0.34	0.08	0.13
	The coefficient of water balance/W	1.22	1.32	1.24
WRF/72h	Nash-Sutcliffe coefficient/C	0.45	0.66	0.44
	Correlation coefficient/R	0.68	0.36	0.75
	Process relative error/P	0.64	0.62	1.29



	Peak flow relative error/E	0.31	0.35	0.45
	The coefficient of water balance/W	1.67	1.54	1.66
WRF/72h after revised	Nash-Sutcliffe coefficient/C	0.52	0.75	0.55
	Correlation coefficient/R	0.75	0.45	0.82
	Process relative error/P	0.53	0.52	0.98
	Peak flow relative error/E	0.11	0.22	0.23
	The coefficient of water balance/W	1.15	1.14	1.25

590

591 Table 3 Evaluation indices of simulated flood event with different model parameters

parameter type	statistical index	201101010	20120101	20130101
Coupling model 24h/originally optimized model parameters	Nash-Sutcliffe coefficient/C	0.75	0.58	0.75
	Correlation coefficient/R	0.93	0.82	0.85
	Process relative error/P	0.23	0.35	0.11
	Peak flow relative error/E	0.08	0.12	0.16
	The coefficient of water balance/W	1.15	1.08	1.12
Coupling model24h /re-optimized model parameters	Nash-Sutcliffe coefficient/C	0.78	0.74	0.87
	Correlation coefficient/R	0.95	0.86	0.87
	Process relative error/P	0.19	0.28	0.09
	Peak flow relative error/E	0.06	0.08	0.12
	The coefficient of water balance/W	1.03	0.95	1.02



Coupling model 48h/originally optimized model parameters	Nash-Sutcliffe coefficient/C	0.64	0.75	0.62
	Correlation coefficient/R	0.82	0.84	0.86
	Process relative error/P	0.45	0.26	0.22
	Peak flow relative error/E	0.34	0.08	0.13
	The coefficient of water balance/W	1.22	1.32	1.24
Coupling model 48h /re-optimized model parameters	Nash-Sutcliffe coefficient/C	0.72	0.75	0.68
	Correlation coefficient/R	0.86	0.87	0.89
	Process relative error/P	0.32	0.22	0.18
	Peak flow relative error/E	0.21	0.06	0.09
	The coefficient of water balance/W	1.05	1.12	1.06
Coupling model 72h/originally optimized model parameters	Nash-Sutcliffe coefficient/C	0.52	0.75	0.55
	Correlation coefficient/R	0.75	0.45	0.82
	Process relative error/P	0.53	0.52	0.98
	Peak flow relative error/E	0.11	0.22	0.23
	The coefficient of water balance/W	1.15	1.14	1.25
Coupling model 72h /re-optimized model parameters	Nash-Sutcliffe coefficient/C	0.62	0.72	0.61
	Correlation coefficient/R	0.78	0.56	0.87
	Process relative error/P	0.38	0.32	0.75
	Peak flow relative error/E	0.09	0.18	0.17
	The coefficient of water balance/W	1.08	1.02	1.05

592

593 Table 4 Evaluation indices of simulated flood event with different lead time

Rain type	statistical index	20120101	20130101
Rain gages	Nash-Sutcliffe coefficient/C	0.82	0.95
	Correlation coefficient/R	0.89	0.92
	Process relative error/P	0.2	0.08
	Peak flow relative error/E	0.05	0.06
	The coefficient of water balance/W	0.8	1.08
WRF/24h	Nash-Sutcliffe coefficient/C	0.74	0.87
	Correlation coefficient/R	0.86	0.87
	Process relative error/P	0.28	0.09



	Peak flow relative error/E	0.08	0.12
	The coefficient of water balance/W	0.95	1.02
WRF/48h	Nash-Sutcliffe coefficient/C	0.63	0.62
	Correlation coefficient/R	0.84	0.86
	Process relative error/P	0.48	0.22
	Peak flow relative error/E	0.12	0.13
	The coefficient of water balance/W	1.32	1.24
WRF/72h	Nash-Sutcliffe coefficient/C	0.56	0.61
	Correlation coefficient/R	0.56	0.87
	Process relative error/P	0.56	0.75
	Peak flow relative error/E	0.18	0.17
	The coefficient of water balance/W	1.54	1.66

594

595



596

597 References

- 598 [1] Abbott, M.B. et al.: An Introduction to the European Hydrologic System-System
599 HydrologueEuropeen, ‘SHE’, a: History and Philosophy of a Physically-based,
600 Distributed Modelling System, *Journal of Hydrology*, 87, 45-59, 1986.
- 601 [2] Abbott, M.B. et al.: An Introduction to the European Hydrologic System-System
602 HydrologueEuropeen, ‘SHE’, b: Structure of a Physically based, distributed
603 modeling System, *Journal of Hydrology*, 87, 61-77, 1986.
- 604 [3] Ahlgrimm, Maike, Richard M. Forbes, Jean-Jacques Morcrette, and Roel A. J.
605 Neggers. ARM’s Impact on Numerical Weather Prediction at ECMWF[J]., 2016,
606 (57):1-12.
- 607 [4] Barnier, B., L. Siefridt, P. Marchesiello. Thermal forcing for a global ocean
608 circulation model using a three-year climatology of ECMWF analyses. *Journal of*
609 *Marine Systems*, 6:363-380, 1995.
- 610 [5] Borga, M., Borga, E.N. Anagnostou, G. Bloschl d, J.D. Creutine. Flash flood
611 forecasting, warning and risk management: the HYDRATE project[J].
612 *Environmental science & policy*, 2011, (14) :834-844.
- 613 [6] Buizza, R., M. Miller and T. N. Palmer. Stochastic representation of model
614 uncertainties in the ECMWF Ensemble Prediction System[J]. *Q. J. R. Meteorol.*
615 *Soc.* 1999, (125): 2887-2908.
- 616 [7] Burnash, R. J. C.. “The NWS river forecast system-catchment modeling.”
617 *Computer models of watershed hydrology*, V. P. Singh, ed., Water Resource
618 Publications, Littleton, Colo., 311–366, 1995.
- 619 [8] Chen, Yangbo. *Liuxihe Model*, China Science and Technology Press, September
620 2009.
- 621 [9] Chen, Yangbo, Ren, Q.W., Huang, F.H., Xu, H.J., and Cluckie, I.: *Liuxihe Model*
622 *and its modeling to river basin flood*, *Journal of Hydrologic*
623 *Engineering*, 16, 33-50, 2011.
- 624 [10] Chen, Yangbo, Yi Dong, Pengcheng Zhang. Study on the method of flood
625 forecasting of small and medium sized catchment, proceeding of the 2013
626 meeting of the Chinese Society of Hydraulic Engineering, 1001-1008, 2013.
- 627 [11] Chen, Yangbo, Ji Li, Huijun Xu. Improving flood forecasting capability of
628 physically based distributed hydrological model by parameter optimization.
629 *Hydrology & Earth System Sciences*, 20, 375-392, 2016.
- 630 [12] Chen, Y., Li, J., Wang, H., Qin, J., and Dong, L.: Large watershed flood
631 forecasting with high resolution distributed hydrological model, *Hydrol. Earth*
632 *Syst. Sci. Discuss.*, doi:10.5194/hess-2016-489, in review, 2016.
- 633 [13] Danish Hydraulic Institute (DHI). MIKE11: A Modeling System for Rivers and
634 Channels User-guide Manual[R]. DHI, 2004.
- 635 [14] Gao, Songying, Lian qiangsun. Inspection and evaluation numerical forecast
636 product of Japan in precipitation forecasting in Dandong[J]. *Meteorological*, 2006,
637 (6):79-83.
- 638 [15] Giard, D. and E. Bazile. Implementation of a New Assimilation Scheme for Soil
639 and Surface Variables in a Global NWP Model[J]. *Monthly weather*
640 *review*. 2000, (128): 997-1015.



- 641 [16]Givati, A., Barry L., Yubao Liu, and Alon Rimmer.Using the WRF Model in an
642 Operational Stream flow Forecast System for the Jordan River[J].,
643 2012,(51):285-299. DOI: 10.1175/JAMC-D-11-082.1.
644 [17]Han, Dawei, Terence Kwong, and Simon Li. Uncertainties in real-time flood
645 forecasting with neural networks[J]. Hydrological. Process, 2007, (21): 223–
646 228 .
647 [18]Hong, S.Y. and Lim, J.. The WRF Single-Moment 6-Class Microphysics Scheme
648 (WSM6)[J]. Journal of the Korean Meteorological Society, 2006, 42(2):129–51.
649 [19]Hong, Song-You, Ji-Woo Lee. Assessment of the WRF model in reproducing a
650 flash-flood heavy rainfall event over Korea[J]. Atmospheric Research, 2009,
651 (93):818–831.
652 [20]Hu, Xiangjun, Jianhong Tao, Fei Zheng, Na Wang, Tiejun Zhang, Shixiang, Liu,
653 and Dacheng Shang. Synopsis the parameterized scheme of physical process of
654 WRF.Gansu Science and Technology,24, 73-75.2008.
655 [21]Huang, Haibo, Chunyan Chen, andWenna Zhu. Impacts of Different Cloud
656 Microphysical Processes and Horizontal Resolutions of WRF Model on
657 Precipitation on Forecast Effect. METEOROLOGICAL SCIENCE AND
658 TECHNOLOGY,39,529-536,2011.
659 [22]Jasper, Karsten, Joachim Gurtz, and Herbert Lang. Advanced flood forecasting in
660 Alpine watersheds by coupling meteorological observations and forecasts with a
661 distributed hydrological model[J]. Journal of Hydrology, 2002, (267) :40–52.
662 [23]Kain, J.S. The Kain-Fritsch convective parameterization: An update. Journal of
663 Applied Meteorology and Climatology 43, 170–181,2004.
664 [24]Kavvas, M., Chen, Z., Dogrul, C., Yoon, J., Ohara, N., Liang, L., Aksoy, H.,
665 Anderson, M., Yoshitani, J., Fukami, K., and Matsuura, T. (2004). "Watershed
666 Environmental Hydrology (WEHY) Model Based on Upscaled Conservation
667 Equations: Hydrologic Module." J. Hydrol. Eng.,2004, 6(450), 450-464.
668 [25]Kouwen, N.:WATFLOOD: A Micro-Computer based Flood Forecasting System
669 based on Real-Time Weather Radar , Canadian Water Resources Journal,
670 13,62-77,1988.
671 [26]Kumar, Anil, J. Dudhia, R. Rotunno, Dev Niyogi and U. C. Mohanty. Analysis of
672 the 26 July 2005 heavy rain event over Mumbai,India using the Weather
673 Research and Forecasting (WRF)model[J]. Quarterly Journal of the royal
674 meteorological society, 200(134):1897-1910.
675 [27]Li, Hongyan, Hanbing Liu, Ximin Yuan, Shukun Liu. The recognition theory of
676 ANN and its application in flood forecasting[J]. Shui Li Xue Bao, 2002, 06:
677 15-19.
678 [28]Li, Yuan, G.H. Lu, Z.Y. Wu, and Jun Shi. Study of a dynamic downscaling
679 scheme for quantitative precipitation forecasting, Remote Sensing and GIS for
680 Hydrology and Water Resources,IAHS Pub.,
681 doi:10.5194/piahs-368-108-2015,108-113,2015.
682 [29]Li, Zechun and Dehui Chen.The development and application of the operational
683 ensemble prediction system at national meteorological center[J]. Journal of
684 Applied Meteorological Science, 2002, (13):1-15.
685 [30]Liang, X., Lettenmaier, D.P., Wood, E.F.,and Burges, S.J.:A simple
686 hydrologically based model of land surface water and energy fluxes for general
687 circulation models, J. Geophys. Res, 99,14415-14428,1994.
688 [31]Liao,Zhenghong,Yangbo Chen, Xu Huijun, Yan Wanling, Ren Qiwei, Parameter
689 Sensitivity Analysis of the Liuxihe Model Based on E-FAST Algorithm, Tropical
690 Geography, 2012, 32(6):606-612.



- 691 [32]Liao, Zhenghong, Yangbo Chen, Xu Huijun, He Jinxiang, Study of Liuxihe Model
692 for flood forecast of Tiantoushui Watershed, Yangtze River, 2012, 43(20): 12-16.
- 693 [33]Lin, Y L, Farley R D, and Orville H D. Bulk parameterization of the snow field in
694 a cloud model. *Journal of Climate and Applied Meteorology*, 22, 1 065-1 092,
695 1983.
- 696 [34], H..Parameter estimation in distributed hydrological catchment modelling using
697 automatic calibration with multiple objectives, *Advances in Water Resources*,
698 26,205-216, 2003.
- 699 [35]Maussion, F., D. Scherer, R. Finkelnburg, J. Richters, W. Yang, and T. Yao. WRF
700 simulation of a precipitation event over the Tibetan Plateau, China – an
701 assessment using remote sensing and ground Observations[J]. *Hydrol. Earth Syst.*
702 *Sci.*, 2011, (15): 1795–1817. doi:10.5194/hess-15-1795-2011.
- 703 [36]Molteni, F., R. Buizza, T.N. Palmer and T. Petroliaji. The ECMWF Ensemble
704 Prediction System: Methodology and validation. *Meteorol. Soc.*, 1996, 122:
705 73-119.
- 706 [37]Moreno, H. A., Enrique R. Vivoni, David J. Gochis. Limits to Flood Forecasting
707 in the Colorado Front Range for Two Summer Convection Periods Using Radar
708 Nowcasting and a Distributed Hydrologic Model[J]. *Journal of*
709 *Hydrometeorology*, 2013, (14) :1075-1097.
- 710 [38]Niu, Junli and Zhihui Yan. The impact on the heavy rain forecast based on
711 physical process of WRF. *SCIENCE & TECHNOLOGY INFORMATION*.23,
712 42-45, 2007. DOI:10.3969/j.issn.1001-9960.2007.23.011.
- 713 [39]Pan, Xiaoduo, Xin Li, Youhua Ran, and Chao Liu. Impact of Underlying Surface
714 Information on WRF Model in Heihe River Basin. *PLATEA*
715 *UMETEOROLOGY*, 31, 657-667, 2012.
- 716 [40]Pennelly, C., Gerhard Reuter, Thomas Flesch. Verification of the WRF model for
717 simulating heavy precipitation in Alberta[J]. *Atmospheric Research*, 135–
718 136, 172–192, 2014.
- 719 [41]Refsgaard, J. C., 1997. “Parameterisation, calibration and validation of distributed
720 hydrological models.” *J. Hydrol.*, 198, 69–97.
- 721 [42]Rutledge, Steven A. and Peter V. Hobbs. The Mesoscale and Microscale Structure
722 and Organization of Clouds and Precipitation in Midlatitude Cyclones. VIII: A
723 Model for the “Seeder-Feeder” Process in Warm-Frontal Rainbands. *JOURNAL*
724 *OF THE ATMOSPHERIC SCIENCES*. 40, 1185-1206, 1983.
- 725 [43]Shafii, M. and Smedt, F. De: Multi-objective calibration of a distributed
726 hydrological model (WetSpa) using a genetic algorithm, *Hydrol. Earth Syst. Sci.*,
727 13, 2137–2149, 2009.
- 728 [44]Sherman, L. K.. “Streamflow from rainfall by the unit-graph method.” *Eng.*
729 *News-Rec.*, 1982, 108, 501–505.
- 730 [45]Shim, Kyu-Cheoul, Darrell G. Fontane, M. ASCE, John W. Labadie, and
731 M. ASCE. Spatial Decision Support System for Integrated River Basin Flood
732 Control. [J]. *Journal of Water Resources Planning and Management*, 2002, 128(3):
733 190-201. DOI: 10.1061/(ASCE)0733-9496(2002)128:3(190)
- 734 [46]Skamarock, William C., Joseph B. Klemp, Jimy Dudhia., David O. Gill, Dale M.
735 Barker, Wei Wang, and Jordan G. Powers. A Description of the Advanced
736 Research WRF Version 2[M]. *NCAR TECHNICAL NOTE*, NCAR/TN–468, STR,
737 2005.
- 738 [47]Skamarock, William C., Joseph B., Klemp Jimy, Dudhia David, O. Gill, Dale M.
739 Barker Michael, G. Duda, Xiangyu, Huang Wei Wang, Jordan G. Powers. A



- 740 Description of the Advanced Research WRF Version 3 [M].NCAR TECHNICAL
741 NOTE, NCAR/TN-468,STR, 2008.
- 742 [48]Takenaka, Hideaki, Takashi Y. Nakajima, Akiko Higurashi, Atsushi
743 Higuchi,TamioTakamura, Rachiel T. Pinker, and Teruyuki Nakajima.Estimation
744 of solar radiation using a neural network based on radiative transfer[J].Journal of
745 Geophysical Research, 116, D08215: 1-26,doi:10.1029/2009JD013337, 2011.
- 746 [49]Tingsanchali, T. Urban flood disaster management [J].Procedia Engineering,
747 2012, (32) :25 -37.
- 748 [50]Toth, E., A. Brath, A. Montanari. Comparison of short-term rainfall prediction
749 models for real-time flood forecasting [J]. Journal of Hydrology,2000, (239):
750 132-147.
- 751 [51]Vieux, B. E., and Vieux, J. E.:VfloTM: A Real-time Distributed Hydrologic
752 Model[A]. In:Proceedings of the 2nd Federal Interagency Hydrologic Modeling
753 Conference, July 28-August 1, Las Vegas, Nevada. Abstract and paper on
754 CD-ROM, 2002.
- 755 [52]Wang, Xiaojun, Hao Ma.Progress of Application of the Weather Research and
756 Forecast (WRF) Model in China. ADVANCES IN EARTH
757 SCIENCE,26,1191-1199,2011.
- 758 [53]Wang, Z., Batelaan, O., De Smedt, F.: A distributed model for water and energy
759 transfer between soil, plants and atmosphere (WetSpa). Journal of Physics
760 andChemistry of the Earth 21, 189-193, 1997.
- 761 [54]Xu, Guoqiang, Xudong Liang, Hui Yu, Liping Huang, and JishanXue.
762 Precipitation Simulation Using Different Cloud-Precipitation Schemes for a
763 Landfall Typhoon.PLATEA UMETEOROLOGY, 26, 891-900, 2007.
- 764 [55]Xu, Huijun, Yangbo Chen, Zeng Biqui, He Jinxiang, Liao Zhenghong,
765 Application of SCE-UA Algorithm to Parameter Optimization of Liuxihe
766 Model,Tropical Geography, 2012.1, 32(1): 32-37.
- 767 [56]Xu, Huijun,Yangbo Chen, Li Zhouyang, He Jinxiang.Analysis on parameter
768 sensitivity of distributed hydrological model based on LH-OAT
769 Method[J].Yangtze River,2012, 43(7): 19-23.
- 770 [57]Zappa, Massimiliano, Keith J. Beven, Michael Bruen, Antonio S. Cofino, Kok,
771 Eric Martin, Pertti Nurmi, Bartlome Orfila, Emmanuel Roulin, Kai Schroter,
772 Alan Seed, Jan Szturc, Bertel Vehvilainen, Urs Germann, and Andrea Rossa.
773 Propagation of uncertainty from observing systems and NWP into hydrological
774 models: COST-731 Working Group 2[J].Atmospheric Science Letters.2010, (11):
775 83-91.
- 776 [58]Zhang, Guocai. Progress of Weather Research and Forecast (WRF) Model and
777 Application in the United States.Meteorological,12, 27-31,2004.
- 778 [59] Zhao, R. J.. Flood forecasting method for humid regions of China, East China
779 College of Hydraulic Engineering, Nanjing, China, 1977.